

Competitive accretion in embedded stellar clusters

I. A. Bonnell¹, M. R. Bate², C. J. Clarke² and J. E. Pringle²

¹ *School of Physics and Astronomy, University of St Andrews, North Haugh, St Andrews, Fife, KY16 9SS.*

² *Institute of Astronomy, Madingley Road, Cambridge CB3 0HA.*

26 April 2024

ABSTRACT

We investigate the physics of gas accretion in young stellar clusters. Accretion in clusters is a dynamic phenomenon as both the stars and the gas respond to the same gravitational potential. Accretion rates are highly non-uniform with stars nearer the centre of the cluster, where gas densities are higher, accreting more than others. This competitive accretion naturally results in both initial mass segregation and a spectrum of stellar masses. Accretion in gas-dominated clusters is well modelled using a tidal-lobe radius instead of the commonly used Bondi-Hoyle accretion radius. This works as both the stellar and gas velocities are under the influence of the same gravitational potential and are thus comparable. The low relative velocity that results means that $R_{\text{tidal}} < R_{\text{BH}}$ in these systems. In contrast, when the stars dominate the potential and are virialised, $R_{\text{BH}} < R_{\text{tidal}}$ and Bondi-Hoyle accretion is a better fit to the accretion rates.

Key words: stars: formation – stars: luminosity function, mass function – open clusters and associations: general.

1 INTRODUCTION

Star formation involves the collapse of molecular cloud cores under their self-gravity through $\gtrsim 20$ orders of magnitude in density. This process is extremely non-homologous in that a small fraction reaches stellar densities while the vast majority of the mass is still infalling (Larson 1969). Thus, a stellar core, comprising a small fraction of a solar mass, is initially formed which grows through the accretion of the infalling envelope. It is the accretion which ultimately determines the final stellar properties (Stahler, Shu & Taam 1980; Palla 1999) as well as the observed characteristics during its pre-main sequence evolution (Henricksen André & Bon-temps 1997; André, Ward-Thompson & Barsony 2000).

Complicating this picture is the fact that most stars do not form in isolation but rather in groups from binary systems (Mathieu et al. 2000) to stellar clusters (Clarke, Bonnell & Hillenbrand 2000). The separation between the individual components of these systems is typically less than the size of an accreting envelope such that they must compete for the reservoir of material.

Surveys of star forming regions have found that the majority of pre-main sequence stars (50 to 90 per cent depending on the region considered) are found in clusters (e.g Lada et al. 1991; Lada, Strom & Myers 1993). These clusters contain anywhere from tens to thousands of stars with typical numbers of around a hundred (Lada et al. 1991; Phelps & Lada 1997; Clarke et al. 2000). Studies of the stellar content of young (ages $\approx 10^6$ years) clusters (e.g. Hillenbrand 1997)

reveal that they contain both low and high-mass stars in a similar proportion to that in a field-star IMF (Hillenbrand 1997). Observations of young clusters have shown that they are usually associated with massive clumps of molecular gas (Lada 1992). Typically, the mass of the gas in the youngest clusters is greater than that in stars (Lada 1991), with up to 90 % of the cluster mass in the form of gas. Gas can thus play a crucial role in the evolution of the clusters. Furthermore, there is a degree of mass segregation present in the clusters with the most massive stars generally found in the cluster cores (Hillenbrand & Hartmann 1998; Carpenter et al. 1997). These systems are generally too young for two-body relaxation to explain these observations implying that mass segregation is an initial condition of stellar clusters (Bonnell & Davies 1998).

Previous studies have explored the physics of accretion in binary systems (Bate & Bonnell 1997; Bate 2000) and in small stellar clusters (Bonnell et al. 1997). Accretion in binary systems plays an important role in determining the system’s mass ratio and separation (Bate 2000). In the more chaotic environment of a small stellar cluster, the accretion rates are highly non-uniform with a few stars accreting much more than the rest. The accretion rates primarily depend on the star’s position within the cluster such that those nearest the centre have the highest accretion rates (Bonnell et al. 1997). This competitive accretion results in a spectrum of stellar masses, from initially equal masses, and as such is a promising candidate for explaining the observed initial mass function (Zinnecker 1982; Bonnell 2000).

In this paper we are extending the work on smaller stellar clusters to larger systems containing up to one hundred stars. The aim is to explore the physics of the competitive accretion in order to get a better grasp of the likely effects of competitive accretion on the spectrum of stellar masses. In § 2 we discuss the numerical calculations. In § 3 we discuss how the accretion is related to the cluster dynamics. Section 4 presents the results on accretion and mass segregation while § 5 presents our results on modelling the physics of competitive accretion. Our conclusions are presented in § 6.

2 CALCULATIONS

The calculations presented here were performed with a hybrid SPH-Nbody code to model the combined presence of stars and gas and their mutual interactions. This code is based on a standard 3-D Smoothed Particle Hydrodynamics (SPH) code (Benz 1990) with gravitational interactions calculated via a tree-code (Benz et al. 1990). The gas is modelled by the normal SPH particles while the stars are modelled using sink-particles (Bate, Bonnell & Price 1995). These sink-particles interact with other particles only through gravitational forces and the accretion of the gaseous SPH particles. The accretion is modelled by removing gas particles within a predetermined radius of one of the sink-particles, providing they are bound to the sink-particle, and adding their mass and momentum to the sink-particle's (Bate et al. 1995). The radius at which this accretion occurs, the sink-radius R_{sink} is chosen to be sufficiently small that it does not overtly affect the gas flow outside this radius. In practice this means that it must be smaller than any physical accretion radius (e.g. Bondi-Hoyle accretion radius) where the gas becomes bound to the star. The sink-radius cannot be too small either as this translates into a prohibitively small time-step. In this study, we use a sink-radius of $R_{\text{sink}} = 10^{-3} \times R_{\text{clust}}$, the initial cluster radius.

The simulations were performed with 10^5 SPH particles to model the gas. The end-point of the simulations was generally chosen to be when roughly half of the SPH particles were accreted, although several were run till all the gas was accreted. The analysis was performed before the majority of the gas was accreted in order to ensure sufficient resolution. Furthermore, several simulations were rerun with accreted particles each replaced by nine lower-mass particles to ensure that the results were not overtly affected by the resolution. This was indeed found to be the case in all the simulations except those with both ‘hot’ gas and stars where the low accretion rates require larger particle numbers to be fully resolved. Limitations of the simulations presented here are that there is no feedback from the stars onto the gas and that the gas does not initially contain any turbulent (or other) motions. These two effects could play a significant role in the cluster evolution and in the accretion process but are beyond the scope of this paper.

2.1 Initial Conditions

We have simulated accretion onto a large number of cluster models to cover the range in possible initial conditions. We present the results from a number of these simulations,

listed in Table 1, in order to illustrate the relevant physical processes of accretion in stellar clusters. The simulations are characterised by the number of stars, the gas fraction, the stellar distribution and the number of Jeans masses in the gas,

$$M_J = \left(\frac{5R_g T}{2G\mu} \right)^{3/2} \left(\frac{4}{3}\pi\rho \right)^{-1/2}, \quad (1)$$

where R_g is the gas constant, G is the gravitational constant, and μ is the mean molecular weight. Other cluster parameters are the initial mean Mach number of the stars and the distribution of stellar masses.

All the clusters considered here are initially spherical and have uniform gas distribution. In all cases, the gas is initially static and has only thermal support. The stars initially have a small virial ratio in all cases. The initial conditions are termed ‘cold’ when they contain at least as many Jeans masses as stars. Such initial conditions are the most likely if the cluster forms through a fragmentation event. An isothermal gas equation of state is used throughout. This means that, in the absence of accretion, the gas will collapse to a singularity in approximately one free-fall time.

The initial spatial distribution of stars is either uniform or $n(t) \propto r^{-2}$ as might be expected after a violent relaxation. One simulation (Run C) was performed with an initial range of stellar masses in order to ascertain the importance of the initial stellar mass distribution.

3 ACCRETION AND CLUSTER DYNAMICS

One of the first things we need to understand in terms of the dynamics of accretion in clusters is the timescale. This sets the mean accretion rate and thus how important accretion can be in setting the final stellar mass. Gas accretion by a star is given by the general formula

$$\dot{M}_* \approx \pi\rho v_{\text{rel}} R_{\text{acc}}^2, \quad (2)$$

where ρ is the gas density and v_{rel} is the relative gas-star velocity and R_{acc} is the accretion radius.

One possible estimate of the accretion timescale is using Bondi-Hoyle accretion (Bondi & Hoyle 1944; Bondi 1952), corresponding to an isolated star accreting from a uniform, non-self-gravitating medium. In this model, the accretion radius is given by

$$R_{\text{BH}} = \frac{C_{\text{BH}} G M_*}{v_{\text{rel}}^2 + c_s^2}, \quad (3)$$

where M_* is the stellar mass, and c_s is the gas sound speed and the constant C_{BH} is generally taken to be $C_{\text{BH}} \approx 2$ (Bondi & Hoyle 1944). This approach neglects the self-gravity of the gas, the presence of other stars, the cluster potential and how these affect the accretion. Estimating the accretion timescale as

$$t_{\text{acc}} = \frac{M_{\text{gas}}}{N\dot{M}_*} \quad (4)$$

the Bondi-Hoyle formalism implies

$$t_{\text{acc}}(\text{BH}) \approx \frac{1}{N} \left(\frac{R_{\text{clust}}}{R_{\text{BH}}} \right)^2 t_{\text{dyn}}. \quad (5)$$

If the cluster is virialised

Run	No. of stars	Gas fraction	stellar dist ^a	$N(M_J)$	Mach no.	Initial masses
Run A	100	90	uniform	120	0.5	equal
Run B	100	90	r^{-2}	2.8	0.2	equal
Run C	100	90	uniform	120	0.5	range
Run D	1	99	—	130	0.2	—
Run E	1	99	—	130	2.	—
Run F	30	82	uniform	110	0.6	equal
Run G	100	90	r^{-2}	120	0.5	equal

Table 1. The initial cluster models used to illustrate the physics of the accretion process are listed by the number of stars in the cluster, the percentage of total mass initially in gas, the stellar distribution, the number of Jeans masses contained in gas, the mean Mach number of the stars and the distribution of initial stellar masses.

$$\frac{R_{\text{clust}}}{R_{\text{BH}}} \approx N, \quad (6)$$

then

$$t_{\text{acc}}(\text{BH}) \approx N t_{\text{dyn}}, \quad (7)$$

where N is the number of stars in a cluster and t_{dyn} is the cluster's dynamical or crossing time. In studies of accretion in small- N clusters (Bonnell et al. 1997), this timescale was found to be much too long as it neglects the motion of the gas in the cluster.

Another possible estimate is obtained by considering how the gas evolves under the cluster potential. Assuming the gas is gravitationally unstable (otherwise it would not have formed stars in the first place), dominates the cluster potential, lacks rotational support and remains isothermal, the gas falls towards the centre of the cluster on the free-fall timescale,

$$t_{\text{ff}} = \sqrt{\frac{3\pi}{32G\rho}}. \quad (8)$$

In the absence of any accretion onto existing stars, the gas collapses and forms an additional star containing all the gas mass in approximately one free-fall time. This sets an upper limit on the accretion timescale as the gas remains distributed in the cluster for no more than approximately one free-fall time.

During the collapse, the gas density increases and the cluster potential becomes deeper. Thus as long as the stars remain inside the gas sphere, the increase in the gas density will increase the accretion rate (equation 2). As the density increases towards infinity on a dynamical timescale, the accretion rate also increases on this timescale till all the gas is accreted (or has formed another star at the cluster centre). Thus, the accretion timescale in a self-gravitating gas is given by

$$t_{\text{acc}} \approx t_{\text{ff}}. \quad (9)$$

Comparing these estimates to the numerical simulations, we find that the accretion occurs on the dynamical timescale as the gas density increases dramatically on this timescale. Figure 1 plots the evolution of the total accreted mass versus time for Run A (a cold cluster containing 100 stars with an initial gas fraction of 90 per cent). The stars initially have a total mass of 0.1. They accrete somewhat slowly over the first half of a free-fall time and only double their mass by $0.8 t_{\text{ff}}$. By $0.95 t_{\text{ff}}$ the stars have accreted all the gas in the cluster and have increased their mean mass tenfold.

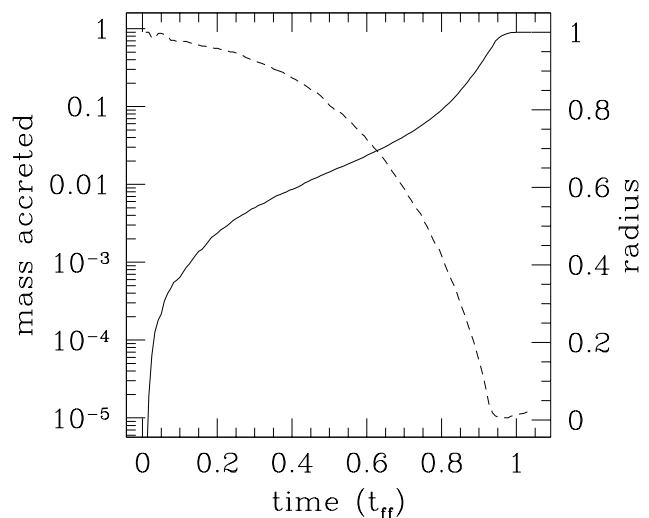


Figure 1. The total accreted mass (solid line) is plotted as a function of time for Run A (a 'cold' cluster containing 100 stars and 90 per cent of its initial mass in the form of gas). The half-mass radius of the stars is also plotted (dashed line). Note that both the gas accretion and the cluster evolution occur on a dynamical timescale.

The half-mass radius of the stellar distribution is also plotted in Figure 1 showing how the cluster evolves on a dynamical timescale. The stars are initially cold and thus in the absence of any gas accretion would revirialise at half their initial radius. Instead, the stars' dynamical evolution is due to the combination of the accretion and the changing cluster potential due to the collapse of the gas. As the gas collapses, the deepening of the cluster potential forces the stars to follow the gas and shrink. Additionally, the accretion increases the stellar masses making them more bound to each other which causes the stellar distribution to shrink further. Thus not only does the accretion occur on a dynamical timescale but the cluster as a whole evolves on this timescale. This evolution may be important in forming massive stars if they cannot accrete, due to their large radiation pressure, past $\approx 10M_{\odot}$. In this case, the cluster shrinkage due to the accretion can be sufficient to induce stellar collisions which form the most massive stars (Bonnell, Bate & Zinnecker 1998). Stellar collisions are not included in the simulations presented here as the finite stellar size is not

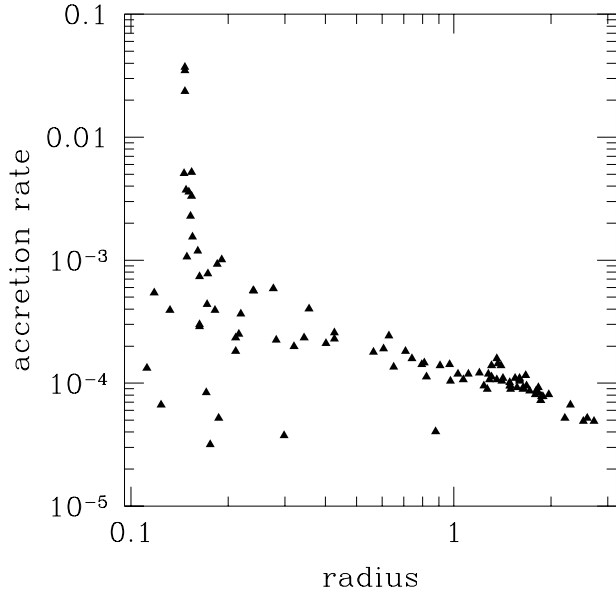


Figure 2. The accretion rate onto 100 stars in a cluster is plotted as a function of the radius in the cluster of each of the stars (Run B). The accretion rates are averaged over $0.1t_{\text{ff}}$ and are calculated at $t \approx 0.65t_{\text{ff}}$. The accretion rate increases towards the centre of the cluster which leads to mass segregation. Initially the cluster is centrally condensed and contains 10 per cent of its mass in stars. The accretion rate is in units of the total cluster mass per t_{ff} .

modelled. The reader is referred to Bonnell et al. (1998) for a discussion on how accretion-induced shrinkage of the cluster can result in stellar collisions.

Although many of the clusters investigated here are cold and contain ≈ 100 Jeans masses, they do not in general collapse to form additional stars. Instead, the gas was accreted onto individual stars that the gas encountered on its way to the cluster centre. Exceptions to this were the simulations run with only one star present in the gas cloud. In these cases the gas can easily collapse to the centre without encountering (being accreted by) the single star.

4 ACCRETION AND MASS SEGREGATION

One of the goals of studying accretion in stellar clusters is to determine if it can explain the initial mass segregation that is observed in young stellar clusters (e.g. Hillenbrand & Hartmann 1998). This segregation of the more massive stars towards the centre of the cluster is not due to two-body relaxation in the cluster as the clusters are often too young (Bonnell & Davies 1998). Moreover, simple Jeans mass arguments imply that the lowest mass stars should be found near the centre of the cluster where the gas density is highest, not the most-massive ones (Zinnecker, McCaughrean & Wilking 1993; Bonnell et al. 1998). Simulations of accretion in small stellar clusters (Bonnell et al. 1997) found that the accretion rate was generally higher for the stars nearer the cluster centre. In this section, we investigate how the accretion rate depends on the stellar positions in the cluster and how this can result in a mass-segregated cluster.

Accretion leads to mass segregation in two ways. Firstly,

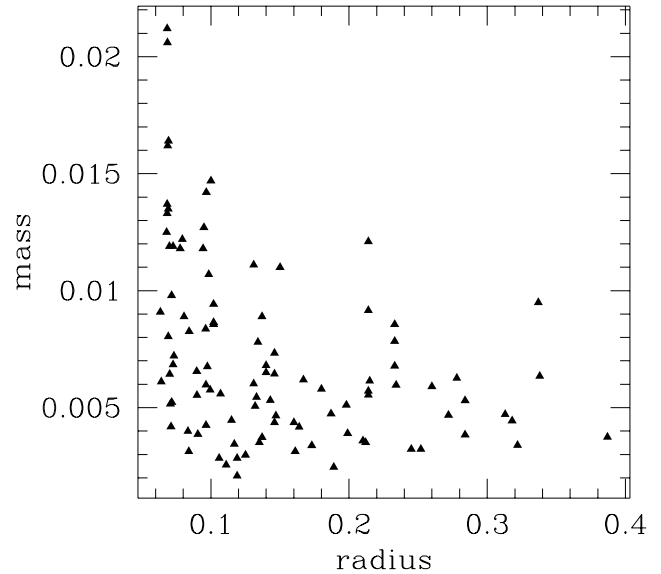


Figure 3. The resultant stellar masses (in units of the total cluster mass) after accretion are plotted as a function of each star's position in the cluster at $t \approx 1t_{\text{ff}}$ for Run A. The initial stellar mass is $m_* = 0.001$. The mass segregation is apparent even though there are significant numbers of low-mass stars near the cluster centre. The cluster is initially uniform and cold and contains 10 per cent of its mass in stars.

as the system relaxes to a centrally-condensed distribution, the gas density increases towards the centre of the cluster which then results in higher accretion rates in the centre than elsewhere. Secondly, mass accretion onto an individual star decreases its kinetic energy (mass loading) which forces it to sink deeper into the cluster potential. Thus, stars that accrete gas sink towards the centre and stars that are in the centre accrete more gas as the density is highest there.

Figure 2 plots the individual accretion rates versus stellar position in the cluster for Run B. These accretion rates are averaged over approximately $0.1t_{\text{ff}}$ at time $t \approx 0.65t_{\text{ff}}$. The 100 stars are initially centrally condensed in this model and the gas, comprising 90 per cent of the total mass, is relatively warm in that it contains only 2.8 Jeans masses. The stars dominate the central part of the potential due to their condensed distribution. Figure 2 shows that the accretion rate increases with decreasing radius with those stars near the cluster centre accreting at a rate more than a hundred times those near the outside. This differential accretion is due to the higher gas densities found near the centre of the cluster and obviously leads to a mass-segregated cluster on the accretion (dynamical) timescale. The most massive stars are the ones that started out nearest the cluster centre. They have the largest accretion rates and will therefore always be nearest the cluster centre (unless ejected by a dynamical interaction).

For clusters whose stars are initially uniformly spatially distributed, the gas density is initially uniform as well and only becomes significantly centrally concentrated on a free-fall timescale. In this situation, it is not necessarily the stars initially nearest the cluster centre which accrete the most. Instead, it is those which, regardless of how close they

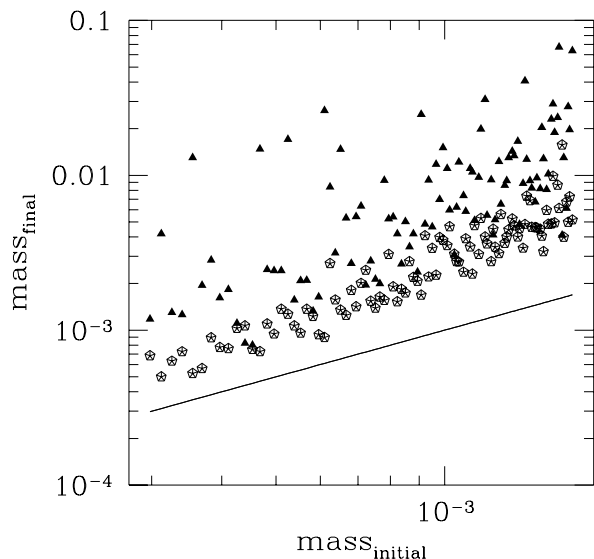


Figure 4. The intermediate ($t \approx 0.87t_{\text{ff}}$, open pentagons) and final ($t \approx 1.0t_{\text{ff}}$, filled triangles) masses are plotted versus the initial stellar mass for Run C, a cluster containing 100 stars with a distribution of initial masses. The solid line denotes the initial range of masses. The cluster is ‘cold’ and contains 90 per cent of its initial mass in the form of gas.

are to the cluster centre, are in a favourable location (e.g. less local competition) that accrete the most. These stars then sink towards the centre and continue to accrete at a higher rate. This still results in a mass segregated cluster but there is no direct correlation between the stars’ *initial* positions in the cluster and their eventual mass. An example of the resulting mass distribution in the cluster is given in Figure 3 for Run A (an initially uniform cluster containing 100 stars with 90 per cent of its mass in the form of cold gas and containing 120 Jeans masses). We note here that although the trend of higher mass stars towards the centre is very distinct, there are still low-mass stars near the cluster centre as is observed in young stellar clusters such as the ONC (Hillenbrand 1997; Hillenbrand & Carpenter 2000).

5 ACCRETION AND STELLAR MASSES

We have shown above that accretion can result in a spectrum of stellar masses and in mass segregation even when the initial mass distribution is that of equal masses. A further question is how dependent the final masses are on the initial mass distribution. We performed a test case with a spread of a factor of five in the initial masses. Figure 4 shows the relationship between the initial and post-accretion stellar masses for Run C, an initially uniform, ‘cold’ cluster with 90 per cent of its mass initially in the form of gas. The post-accretion mass distribution is shown when the stars have increased their total mass (from 10 per cent) to 25 per cent and 100 per cent of the cluster mass. We see that the initial masses play a large role in determining the masses at the intermediate stage, ie that there is still a strong correlation between initial and post accreted masses. On the contrary, at the later stage where the stars have accreted all the gas,

the correlation between final and initial masses is much less clear. There is still a general trend that the mean final mass increases with the initial mass, but the scatter at any given initial mass is so large (a factor 20) that a star’s final mass places only the weakest constraints on the initial mass of the condensation from which it formed.

The reason for this difference in the intermediate and final mass distribution lies in the cluster evolution. The cluster is initially uniform (constant density) such that the only difference in the accretion rates comes from the accretion radius. This is dependent on the stellar masses (see below) and as such leads to a dependence of the post-accretion mass on the initial mass. The cluster is unstable in a uniform configuration and evolves (in this case due to gravitational collapse) to a more centrally-condensed configuration. Once the cluster is centrally condensed, the gas density play a more important role in the accretion rate such that the mass accreted is more due to the gas density than due to the accretion radius. This is especially so if the accretion radius is only weakly dependent on the star’s mass as we shall see below. Thus, a centrally-concentrated cluster allows even initially lower-mass stars to have higher accretion rates, and eventually attain higher masses if they are in regions with high gas density.

6 AN ANALYTIC PRESCRIPTION FOR COMPETITIVE ACCRETION

In addition to seeing how accretion results in mass segregation and a mass spectrum (Figure 3), one of our goals is to understand the physics of the accretion process. This involves determining what sets the accretion rates of individual stars. A parametrised form for the accretion rates will allow the accretion process to be applied to larger groups of stars without needing to resolve the accretion flow around each star.

The first possible parametrisation of the accretion rate is the Bondi-Hoyle formalism discussed above. In this case, the accretion radius is basically the radius where the gravitational energy due to the star is larger than the kinetic energy (including the unperturbed gas velocity relative to the star, v_{rel} , and sound speed, c_s). Thus (Bondi & Hoyle 1944),

$$R_{\text{BH}} = \frac{2GM_*}{v_{\text{rel}}^2 + c_s^2}, \quad (10)$$

and

$$\dot{M}_* \approx \pi \rho \sqrt{v_{\text{rel}}^2 + c_s^2} R_{\text{BH}}^2. \quad (11)$$

Alternatively, the cluster potential sets another radius, the tidal radius, due to the multiple gravitational sources. This radius is analogous to the Roche-lobe radius in accreting binary systems. We adopt this radius as our second potential accretion radius. This tidal-lobe radius is

$$R_{\text{tidal}} = C_{\text{tidal}} \left(\frac{M_*}{M_{\text{enc}}} \right)^{1/3} r_*, \quad (12)$$

where M_* is the star’s mass, and M_{enc} is the mass enclosed within the cluster at the star’s position r_* . In the Roche-lobe approximation, $C_{\text{tidal}} \approx 0.5$ (e.g. Pacynski 1971) which we will adopt throughout this paper. The accretion rate is then

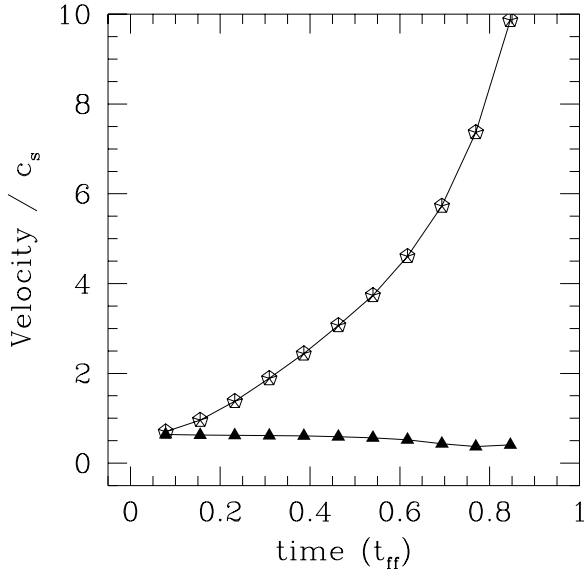


Figure 5. The stellar velocity dispersion (open pentagons) and the mean relative gas velocity in the tidal-lobes of the individual stars (filled triangles) are plotted in units of the gas sound speed c_s as a function of time for Run A. The cluster contains 100 stars, is initially uniform (stars and gas) and contains 90 per cent of its mass in gas (120 Jeans masses).

$$\dot{M}_* \approx \pi \rho v_{\text{rel}} R_{\text{tidal}}^2. \quad (13)$$

The expectation is that the smaller of the two radii should determine the accretion rate as it will be this radius which ultimately decides if the gas is bound to the star and thus will be accreted. Considering the high stellar velocities in a cluster, the Bondi-Hoyle radius is commonly expected to be the smaller of the two.

One difficulty is estimating the relative velocity which goes into both the Bondi-Hoyle radius (equation 10) and the Bondi-Hoyle accretion rate (equation 11). We make two estimates of this velocity, one calculated as the velocity of each star relative to the centre of mass of the cluster and the second is the velocity relative to the gas at the tidal-lobe radius. This relative velocity is calculated by averaging each component of the three-dimensional velocity vectors of the particles which overlap the tidal radius. We shall refer to the Bondi-Hoyle accretion estimate using this relative velocity as the *modified* Bondi-Hoyle accretion. The evolution of each of these velocities is shown in Figure 5 for Run A, a cold cluster of 100 stars initially comprising 10 per cent of the total mass. Both velocities are initially subsonic but the stellar velocities quickly become supersonic as the cluster collapses. In contrast, the relative gas velocity at the tidal-lobe remains subsonic throughout the evolution. This occurs as the gas is accelerated under the same potential that the stars are. Thus, the gas tracks the stellar motions and the relative velocity is small.

The gas density is also estimated at the tidal-lobe radius as that is the radius at which the density is unaffected by the star’s potential. This density is calculated as the average over the particles which overlap the tidal radius. Estimates of the gas density and relative velocity at the tidal-radius are generally well determined as the number of SPH particles

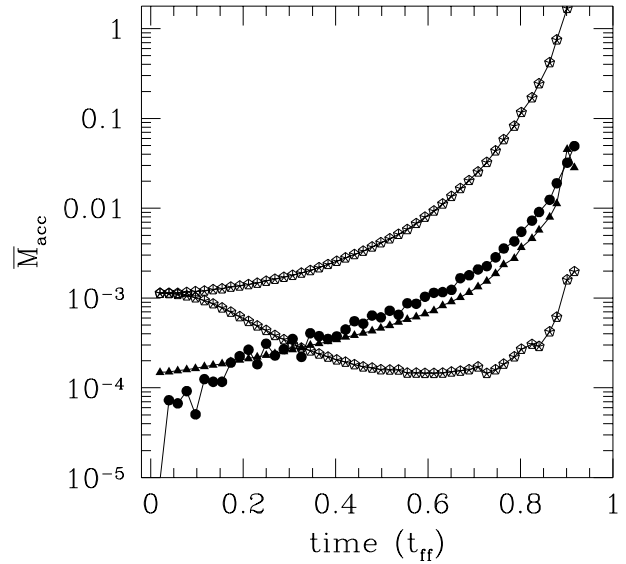


Figure 6. The mean accretion rate (filled circles) is plotted as a function of time for Run A, a cluster of 100 stars which initially has 90 per cent of its mass in gas and is cold. Estimates of the accretion using tidal-lobe as the accretion radius (filled triangles) and using the Bondi-Hoyle radius (open pentagons) are also plotted. The upper Bondi-Hoyle curve uses the relative gas velocity in each star’s tidal lobe (modified Bondi-Hoyle) whereas the bottom curve uses each star’s velocity in the cluster.

there is typically large. Exceptions to this occur when a star is ejected from the cluster and the gas density falls to zero. Another problem that was encountered was due to the presence of other stars in the tidal-lobes. The tidal-lobe formulation does not allow for the effects of close binary systems (with $R_{\text{sep}} < R_{\text{tidal}}$) so that the gas velocities and density do not correspond to only one star. Such systems are generally excluded from the analysis that follows (except in § 6.3).

Using the above estimates of the accretion rate as a function of the local gas density, relative stellar velocity and the accretion radius, we can compare these with the accretion rate determined from the SPH simulations. Figure 6 plots the evolution of the mean accretion rate for Run A, a ‘cold’ cluster of 100 stars where 90 per cent of the initial cluster mass is in the form of gas. Only those stars not in binaries are included. The comparison includes two estimates of the Bondi-Hoyle radius using each star’s velocity relative to the cluster’s centre of mass and its velocity relative to the gas in the tidal-lobe.

The mean accretion rate determined by the SPH simulations increases with time until near the end of the simulation when the gas is significantly depleted. The Bondi-Hoyle accretion rates are both initially much higher than the SPH accretion rate as the stars are initially at rest and the gas is cold. The modified Bondi-Hoyle accretion rate (using the velocity relative to the local gas) remains much higher than the SPH accretion rate. This is because, as shown in Figure 5, this velocity remains subsonic throughout the simulation, and thus $R_{\text{BH}} > R_{\text{tidal}}$. On the other hand, the Bondi-Hoyle accretion rate using the stellar velocity relative to the

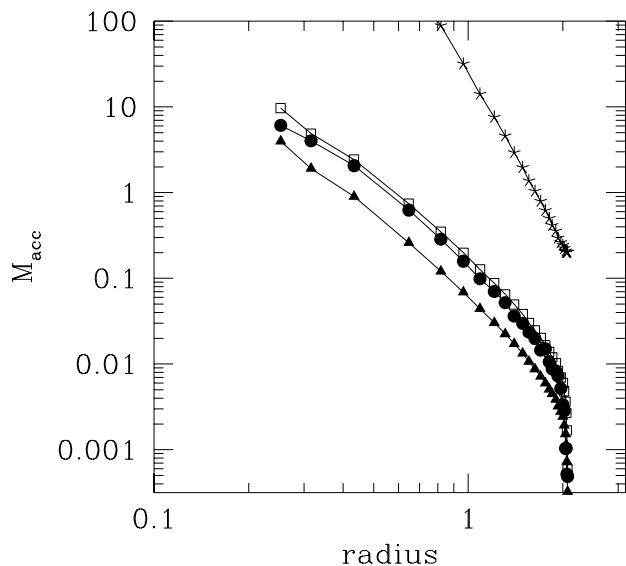


Figure 7. The accretion rate (filled circles) of a single star in a cloud of cold gas is plotted as a function of its radius in the cloud (Run D). The star initially contains one percent of the total mass. Estimates of the accretion rate based on the tidal-lobe (filled triangles) and modified Bondi-Hoyle (stars) are also plotted. The open squares denote the tidal-lobe accretion that includes a component of spherically-symmetric infall.

cluster centre of mass decreases as the stars accelerate and move supersonically. The accretion rate is thereafter significantly smaller than the SPH accretion rate. In contrast, the tidal-lobe accretion rate is generally very similar to the SPH accretion rate throughout the simulation.

From this comparison we can see that the Bondi-Hoyle accretion rate is either too high or too low depending on which velocity is used. It is also readily apparent why the naive accretion rate discussed in Section 3 gives a timescale that is too long. The stellar velocity relative to the cluster’s centre of mass is not the appropriate velocity. It is the velocity relative to the local gas from which the star is accreting which must be used. Thus, from now on, we shall discuss only the modified Bondi-Hoyle accretion rate using the stellar velocity relative to the local gas.

6.1 Single-star clusters

In order to ensure that we can correctly model the accretion rate, we need to compare the different parametrisations of the accretion for individual stars. Figure 7 plots the accretion rate onto one star in a cold gas cloud where 99 per cent of the initial mass is in the form of gas (Run D). Thus, the gas provides the potential as would do an entire cluster but without the difficulties of binary systems and also with increased numerical resolution. The accretion rate onto the star is plotted as a function of its position (radius) in the gas cloud. The accretion rate increases as the star falls in towards the centre of the cloud, due to the increased density there as the cloud collapses to a centrally-condensed configuration. Also plotted in Figure 7 are the modified Bondi-Hoyle accretion rate (using the velocity relative to the gas)

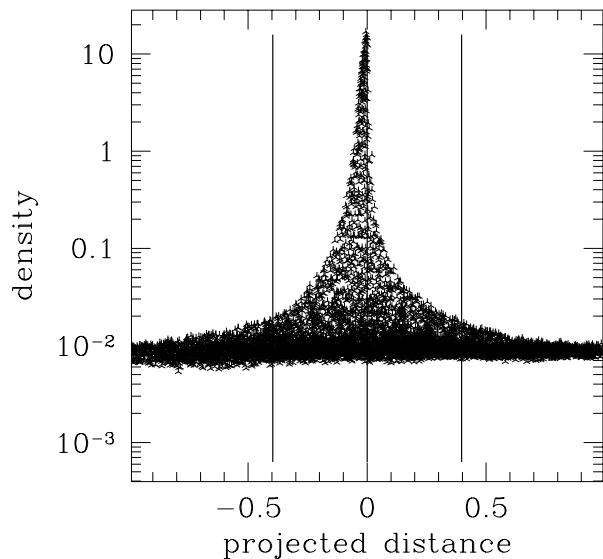


Figure 8. The density of SPH gas particles around a single-star cluster (Run E) are plotted as a function of the projected distance relative to the direction of the star’s motion. The star is travelling inwards at Mach 0.9 relative to the local gas. The size of the tidal lobe is indicated and corresponds approximately to where the density starts to increase towards the star. The modified Bondi-Hoyle radius is larger than the plotted region ($R_{\text{BH}} \approx 2$). Note that the gas density is higher at projected distances < 0 , indicating that the gas is predominantly accreted from behind the star. The slight density gradient is because the star is infalling a bit faster than the gas and thus seeing the higher density ahead.

and two estimates of the tidal-lobe accretion rate. The first of these estimates includes only the relative gas velocity, v_{rel} , whereas the second (and higher) estimate includes an adhoc estimate of the degree of spherical infall through the tidal-lobe, v_{inf} . This spherical accretion can occur over 4π steradians, but, as a first approximation, we use an intermediate value of 3π as the accretion is not completely spherical. Thus

$$\dot{M}_* = \pi \rho R_{\text{acc}}^2 (v_{\text{rel}} + 3v_{\text{inf}}), \quad (14)$$

where v_{inf} is the mean infall velocity of particles at the tidal-lobe radius, $v_{\text{inf}} = \mathbf{v} \cdot \mathbf{r}/|\mathbf{r}|$.

As seen above, the modified Bondi-Hoyle accretion rate is much larger than the SPH accretion rate. The tidal-lobe estimates are much closer to the numerically determined value. The estimate not including spherical infall is slightly lower than the SPH value whereas the estimate including the spherical accretion is very slightly higher than the SPH value.

The tidal-lobe accretion is a good fit to the accretion rate even in simulations where the star is initially supersonic relative to the cluster’s centre of mass. This occurs due to the convergence of the stellar and gas velocities as the cluster collapses. Both the star’s and the gas velocities are increasingly dominated by the gravitational acceleration of the cluster. As both the star and the gas start collapsing towards the centre of the system, the gas velocity inside the star’s tidal-lobe becomes more similar to the star’s velocity. Thus, the relative velocity decreases and the flow

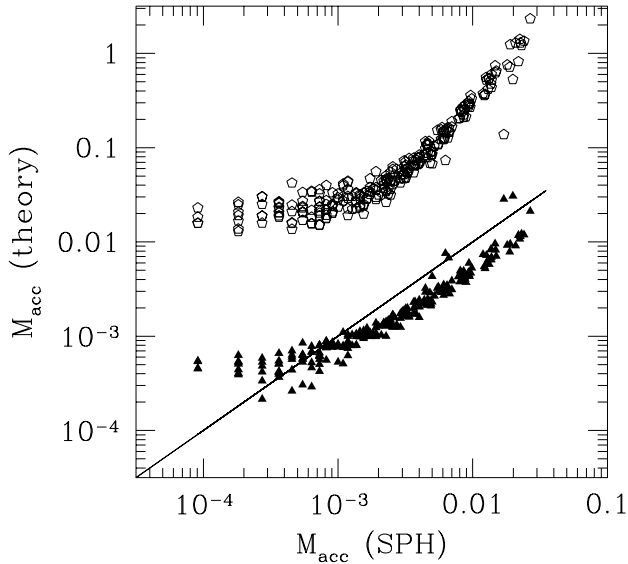


Figure 9. Estimates of the accretion rate using the modified Bondi-Hoyle (open pentagons) and tidal-lobe (filled triangles) formalisms are plotted against the SPH determined accretion rates for each star in a cluster of 30 (Run F). Only stars that do not have companions within R_{tidal} are included. The cluster is initially uniform, cold and contains 82 per cent of its mass in gas.

becomes subsonic. This effect is aided by the accretion as it helps converge the star’s velocity to that of the flow. Thus, $R_{\text{tidal}} < R_{\text{BH}}$ and the tidal-lobe accretion determines the accretion rate.

The finding that the tidal-lobe radius is a good approximation to the accretion radius is further backed up by looking at the gas density near the accreting star. Figure 8 plots the gas density as a function of the projected distance from the star for a single-star initially travelling at Mach 2 in a cluster potential dominated by gas (Run E). Figure 8 is plotted at a time by which the gravitational acceleration of the cluster has converged the stellar and gas motions such that both the star and the gas are moving inwards and the relative velocity of the local gas is Mach 0.9. The projected distance is calculated as the distance relative to the star’s velocity,

$$d_{\text{proj}} = \frac{\mathbf{r} \cdot \mathbf{v}}{|\mathbf{v}|}. \quad (15)$$

We see that the gas density starts to increase at a distance that corresponds roughly to the tidal-lobe radius as expected if this is the physical accretion radius. It is also worth noting that the gas density is somewhat skewed relative to the star’s position with higher density material at greater distances behind the star than in front of it (relative to its motion). This occurs as generally the material is accreted from behind the star, as in the classical Bondi-Hoyle accretion.

6.2 Many-star clusters

Accretion onto stellar clusters is considerably more complex than the above models of a single star in a gas-dominated potential. In a stellar cluster, accretion is not only limited

by the tidal potential of the overall cluster but also by competitive accretion from other stars. Figure 9 plots the comparison of the SPH accretion rate with that based upon tidal-lobe and modified Bondi-Hoyle accretion for Run F, a ‘cold’ cluster of 30 stars initially containing 82 per cent of its mass in gas. The accretion rates are plotted for all stars that do not have another star within their tidal-lobe. This is done as the tidal-lobe determination neglects the presence of any companions (the effect of other stars in the tidal-lobe is discussed in §6.3).

The evolution of the accretion rate for the cluster is from low accretion rates towards higher accretion rates as the cluster collapses under its self-gravity. The quantisation of the lowest accretion rates is due to numerical accuracy and therefore no conclusions are based upon these points. We see that, as in the case of the single-star cluster, the tidal-lobe accretion is a good approximation to the numerical accretion rate determined by the SPH code. In contrast, the modified Bondi-Hoyle accretion rate, using the relative velocity inside the tidal-lobe, is much too high. It is important to note that the tidal-lobe accretion is a good approximation to the SPH determined accretion rate, although it generally slightly underestimates it. In contrast, not only is the modified Bondi-Hoyle accretion rate too high, it also diverges from the numerical accretion rate towards the higher accretion rates. The tidal-lobe accretion is a better fit to the accretion rate as $R_{\text{tidal}} < R_{\text{BH}}$ when the local gas velocity is used to calculate R_{BH} .

This agreement between the numerical and tidal-lobe accretion rates was found for most clusters as long as the gas is reasonably cold. If the gas is sufficiently warm then $R_{\text{BH}} < R_{\text{tidal}}$ and the Bondi-Hoyle is a reasonable fit to the accretion. Such a situation occurs if the gas contains only a few Jeans masses and thus should not have been able to fragment to form the number of stars found in the cluster. One possibility for a cluster with relatively warm gas is when feedback from young stars heats up the gas. Other exceptions were found when many stars are in the same tidal-lobe such as occurs when gas infalls from outside the cluster onto a star-dominated potential, and virialised cluster (see below). Generally up to a third of systems have an other star within their tidal-lobes at any given time, although this can be significantly higher in the stellar dominated potentials. In this last case, most of the stars have $R_{\text{BH}} < R_{\text{tidal}}$ although some are still better modelled by the tidal-lobe accretion when their velocities are inwards.

6.3 Accretion in a stellar dominated potential

As noted above, companions within a star’s tidal-lobe complicate the competitive accretion picture. This becomes increasingly important during the evolution as the gas is accreted and the stars come, at least in the centre, to dominate the cluster potential. In such circumstances, companion stars in each other’s tidal-lobes becomes common. In such circumstances the tidal-lobe accretion formalism as described above does not work as the mass crossing into an individual tidal-lobe can still be accreted by several objects.

When a star has one or more companions inside its nominal tidal-lobe, it’s velocity can be significantly higher than the surrounding gas as it is under the additional acceleration of the relatively close companion(s). The extreme of this is

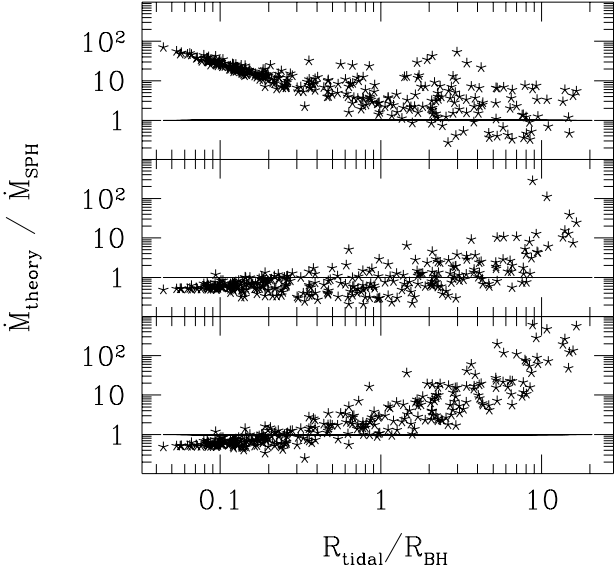


Figure 10. The ratio of the theoretical accretion rates compared to that calculated by the SPH code is plotted against the ratio of the tidal-lobe radius to the modified Bondi-Hoyle radius for Run C. The top panel uses the modified Bondi-Hoyle accretion radius whereas the bottom panel uses the tidal-lobe radius as the accretion radius. The middle panel uses the tidal-lobe accretion radius but adapted to include the effects of multiple stars inside this radius (see text). The tidal-lobe radius gives a better fit to the accretion rate when $R_{\text{tidal}} \lesssim R_{\text{BH}}$. The accretion rates are calculated for a cluster of 100 stars with variable initial masses and an initial gas fraction of 90 per cent.

when the gas is falling onto a virialised cluster and hence the stellar and gas velocities are generally uncorrelated. In this case, the modified Bondi-Hoyle radius becomes smaller than the tidal-lobe radius ($R_{\text{BH}} < R_{\text{tidal}}$) and thus determines the accretion rate. Figure 10 plots the ratio of the theoretical to numerical accretion rates versus the ratio of the tidal-lobe radius to the modified Bondi-Hoyle radius for Run C. The tidal-lobe accretion (bottom panel) models well the accretion rate when the tidal-lobe is smaller than the modified Bondi-Hoyle radius ($R_{\text{tidal}}/R_{\text{BH}} \lesssim 1$). When the tidal-lobe is significantly larger than the modified Bondi-Hoyle radius, as is the case when other stars are present inside the tidal-lobe, then the tidal-lobe formalism seriously overestimates the accretion rate. The top panel of Figure 10 shows the case when modified Bondi-Hoyle accretion is used. As found above, the modified Bondi-Hoyle formalism seriously overestimates the accretion rate when $R_{\text{tidal}}/R_{\text{BH}} \lesssim 1$ as the accretion is determined by the size of the tidal-lobe. In contrast, the modified Bondi-Hoyle formalism works better than the tidal-lobe formalism when $R_{\text{tidal}} \gg R_{\text{BH}}$. The scatter towards the right of each panel in Figure 10 is due to numerical resolution (low accretion rates) and sampling as the effective accretion radius becomes small (few particles to calculate v_{rel}, ρ).

The middle panel of Figure 10 shows the result when tidal-lobe accretion is adapted to include the effects of companions. This is done by estimating the fraction of the material entering the tidal-lobe which is accreted by the star. In the tidal-lobe formalism, this can be calculated by modifying equation (13) as

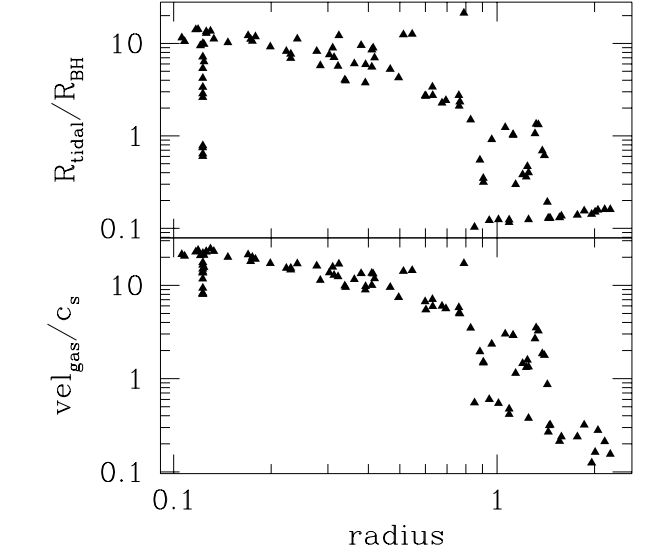


Figure 11. The Mach number of the relative gas flow near each star is plotted as a function of the stars' positions in the cluster for Run G (lower panel). The upper panel shows the corresponding ratio of the tidal-lobe radius to modified Bondi-Hoyle radius as a function of position in the cluster. The stars dominate the inner parts of the cluster such that the stellar and gas velocities are uncorrelated, resulting in $R_{\text{tidal}} > R_{\text{BH}}$. The gas dominates the outer parts of the cluster such that the gas and stellar velocities are correlated and $R_{\text{tidal}} < R_{\text{BH}}$. The values are averaged over $\approx 0.1t_{\text{ff}}$ at $t \approx 1.0t_{\text{ff}}$. The relative overdensity of stars at $r \approx 0.12$ indicates that the deepest part of the cluster potential, where the most massive stars are, is not at the centre of mass of the system.

$$\dot{M}_* = \pi \rho v_{\text{inf}} \left(\frac{M_*^2}{\sum_{i=1}^{N_{\text{comp}}} M_i^2} \right) R_{\text{tidal}}^2 \quad (16)$$

where v_{inf} is the mean spherical infall through the tidal-lobe, and N_{comp} is the number of stars in R_{tidal} . The mass term effectively recalculates the cross-section of the tidal-lobe to include the companions (as $R_{\text{tidal}}^2 \propto (M_*/M_{\text{enc}})^{1/3}$), while using v_{inf} removes the effect of the orbital velocity as the stars move around each other inside the tidal-lobe. We see this estimate of the tidal-lobe accretion works fairly well for $R_{\text{tidal}} \lesssim 10R_{\text{BH}}$, and models to first order the reduction in the accretion rates due to companions inside the tidal-lobe. The limitation of this approach is that it neglects the individual velocities of the stars which will modify the accretion rates. Thus, once $R_{\text{tidal}} \gg R_{\text{BH}}$ we are left with using the modified Bondi-Hoyle formalism.

As a stellar cluster accretes from the gas, the mass-fraction in the stars increases while it decreases for the gas. Once the stars dominate the cluster potential, their evolution is no longer determined primarily by the collapsing gas. They then virialise and thus have velocities uncorrelated to the infalling gas. This transition is illustrated in Figure 11 showing the relative gas velocity as a function of stellar position for Run G. The stars are initially centrally condensed which results in their dominating the central portions of the cluster potential. In the outer regions of the cluster, the ‘cold’ gas still dominates the potential such that both stars and gas are infalling and the relative gas velocity is subsonic.

Inside of $r = 0.9$, the gas contributes less than 25 per cent of the mass and thus no longer determines the dynamics. The stars become virialised and the relative gas velocities are large as the stellar and gas motions are uncorrelated. Figure 11 also plots the ratio of the tidal-lobe radius to the modified Bondi-Hoyle radius as a function of position in the cluster. Stars exterior to $r = 0.9$ have $R_{\text{tidal}} \lesssim R_{\text{BH}}$ as the relative gas velocities are subsonic whereas stars interior to $r = 0.9$ have $R_{\text{tidal}} > R_{\text{BH}}$ as the relative gas velocities are supersonic. Exceptions to this are the most massive stars in the centre of the cluster which, due to their high mass, have low velocities and thus $R_{\text{tidal}} \lesssim R_{\text{BH}}$ once again.

In general as a cluster accretes from its gas reservoir, the stars begin to dominate the potential from the inside out. This occurs due to the higher accretion rates in the centre and due to the settling of the accreting stars. Thus, as the gas infalls from larger radii onto the cluster it will pass through two regimes. First, where the gas dominates the potential, and the stellar dynamics, the accretion is dominated by the tidal-lobes of each star. Second, further in where the stars dominate the potential and are virialised, the accretion is determined by a Bondi-Hoyle accretion.

7 DISCUSSION OF ACCRETION MODELLING

In the above sections, we found that gas accretion in stellar clusters is generally well modelled by using the tidal-lobe as the accretion radius. This formalism works as the cluster dynamics are dominated by the overall collapse of the cluster due to its self-gravity. In this case the gas in the tidal lobe of a star has a similar velocity to the star as both are primarily due to the same gravitational acceleration. This results in a large modified Bondi-Hoyle radius such that the smaller tidal-lobe radius dominates the accretion, $R_{\text{acc}} \approx R_{\text{tidal}} < R_{\text{BH}}$. Such a scenario will always result when the gas dominates the gravitational potential and is dynamically moving under the influence of its self-gravity. In such a case, even if the stars are initially virialised, the changing potential and the gas accretion will maintain similar gas and stellar velocities.

Complications arise when more than one star is in a tidal-lobe region as this increases the stellar velocity relative to the gas velocity in the tidal-lobe. Gas accretion can then be modelled by including the additional stars in the calculation of the tidal-lobe (and thus the accretion cross section). Once the stars dominate the gravitational potential and are virialised, then $R_{\text{tidal}} \gg R_{\text{BH}}$ and accretion of infalling gas can be well modelled with modified Bondi-Hoyle accretion although some care has to be taken to calculate the appropriate density and velocity of the gas.

8 CONCLUSIONS

We find that accretion in stellar clusters occurs on a dynamical timescale. Both the gas and stellar motions are governed by the cluster's gravitational potential. This ensures that the gas will fill the depleted areas and thus find the stars onto which it accretes.

In clusters where gas dominates the potential, the accretion process is better modelled by using the tidal-lobe

radius, R_{tidal} , as the accretion radius rather than the commonly used Bondi-Hoyle radius, R_{BH} . This works as both the stellar and gas velocities are dominated by the gas-dominated gravitational potential, and thus have similar velocities. In this case, we have $R_{\text{tidal}} \lesssim R_{\text{BH}}$ and the smaller R_{tidal} determines the accretion rate. This will occur as long as the gas is the dominant component and is free to collapse (is unsupported against gravity). In contrast, where the stars dominate the cluster potential and are virialised, the stellar and gas velocities are uncorrelated resulting in high relative gas velocities and $R_{\text{BH}} < R_{\text{tidal}}$. In this case the accretion is better modelled by Bondi-Hoyle accretion.

Accretion in a stellar cluster is highly non-uniform with different stars accreting at significantly different rates. Coupling this with a large mass fraction in the form of gas in the cluster results in a spectrum of stellar masses, even from initially equal masses. The accretion rate depends primarily on the local gas density and thus on the star's position in the cluster as the gas quickly concentrates towards the deepest part of the potential well. There is a weak dependence on the mass ($M_* \propto M_*^{2/3}$ for tidal-lobe accretion) such that lower initial masses bias against accretion. This can be overwhelmed by higher gas densities found in the centre of the cluster. Thus, competitive accretion naturally results in a mass-segregated cluster on the formation timescale and does not require subsequent two-body relaxation.

9 ACKNOWLEDGEMENTS

We thank Hans Zinnecker for useful discussions and continual enthusiasm. IAB acknowledges support from a PPARC advanced fellowship.

REFERENCES

- André P., Ward-Thompson D., Barsony M., 2000, in *Protostars and Planets IV*, eds V. Mannings, A. P. Boss and S. S. Russell (Tucson: University of Arizona Press), p. 59
- Bate M.R., 2000, MNRAS, 314, 33
- Bate M. R., Bonnell I. A., 1997, MNRAS, 285, 33
- Bate M. R., Bonnell I. A., Price N. M., 1995, MNRAS, 277, 362
- Benz W., 1990, in Buchler J.R., ed., *The Numerical Modelling of Nonlinear Stellar Pulsations*. Kluwer, Dordrecht, p. 269
- Benz W., Bowers R. L., Cameron A. G. W., Press W., 1990, ApJ, 348, 647
- Bondi H., 1952, MNRAS, 112, 195
- Bondi H., Hoyle F., 1944, MNRAS, 104, 273
- Bonnell I.A., 2000, in *Star formation from the small to the large scale*, eds F. Favata, A. Kaas and A. Wislon, ESA SP-445, in press
- Bonnell I. A., Bate M. R., Clarke C. J., Pringle J. E., 1997, MNRAS, 285, 201
- Bonnell I. A., Bate M. R., Zinnecker H., 1998, MNRAS, 298, 93
- Bonnell I. A., Davies M.B., 1998, MNRAS, 295, 691
- Carpenter, J. M., Meyer, M. R., Dougados, C., Strom, S. E., Hillenbrand, L. A., 1997, AJ, 114, 198
- Clarke C.J., Bonnell I.A., Hillenbrand L.A., 2000, in *Protostars and Planets IV*, eds V. Mannings, A. P. Boss and S. S. Russell (Tucson: University of Arizona Press), p. 151
- Henricksen R.N., André P., Bontemps S., 1997, A&A, 323, 549
- Hillenbrand L. A., 1997, AJ, 113, 1733
- Hillenbrand L. A., Carpenter J. M., 2000 ApJ, August 20 issue
- Hillenbrand L. A., Hartmann L., 1998, ApJ, 492, 540

- Lada E. A., 1992, *ApJL*, 393, 25L
- Lada E. A., Depoy D. L., Evans N. J. Gatley I. 1991, *ApJ*, 371
171
- Lada E., Strom S., Myers P., 1993, in *Protostars and Planets III*,
eds E. Levy, J. Lunine, University of Arizona, p. 245
- Larson R. B., 1969, *MNRAS*, 145, 271
- Lynden-Bell D., 1967, *MNRAS*, 136, 101
- Mathieu R.D., Ghez A.M., Jenson E.L.N., Simon M., 2000, in
Protostars and Planets IV, eds V. Mannings, A. P. Boss and
S. S. Russell (Tucson: University of Arizona Press), p. 703
- Meyer M., Lada E. A., 1999, in *The Orion Nebula Revisited*, M.
McCaughrean and A. Burkert (eds), in press
- Pacynski B. 1971, *ARA&A*, 9, 183
- Palla F., 1999, in *The Origin of Stars and Planetary Systems*, C.
Lada and N. Kyfalis (eds),(Kluwer) p. 375
- Phelps, R., Lada, E., 1997, *ApJ*, 477, 176
- Ruffert M., 1996, *A&A*, 311, 817
- Stahler S.W., Shu F.H., Taam R.E., 1980, *ApJ*, 241, 637
- Zinnecker H., 1982 in *Symposium on the Orion Nebula to Honour
Henry Draper*, eds A. E. Glassgold et al., New York Academy
of Sciences, p. 226
- Zinnecker H., McCaughrean M. J., Wilking B. A., 1993 in *Proto-
stars and Planets III*, eds E. Levy and J. Lunine, University
of Arizona, p. 429